Calibration of Na partitioning in the calcitic foraminifer *Operculina ammonoides* under variable Ca concentration: Toward reconstructing past seawater composition

Hagar Hauzer[1], David Evans[2,3], Wolfgang Müller[4,5], Yair Rosenthal[6], Jonathan Erez[1]

Corresponding author: Hagar.Hauzer@mail.huji.ac.il

1. Institute of Earth Sciences, the Hebrew University, Jerusalem, Israel
2. Department of Geology and Geophysics, Yale University, New Haven, Connecticut, USA
3. School of Earth and Environmental Sciences, University of St Andrews, St Andrews, UK
4. Department of Earth Sciences, Royal Holloway University of London, Egham, UK
5. Institute of Geosciences, Goethe University, Frankfurt, Germany
6. Department of Marine and Coastal Sciences and Department of Earth and Planetary Sciences, Rutgers University, New Brunswick, USA

Keywords: seawater calcium proxy, Na/Ca calibration, live-foraminifera, ocean paleochemistry

Abstract

Reconstructions of past changes in the seawater calcium concentration (Ca_{sw}) are critical for understanding long-term changes in the carbon cycle and for accurate application of elemental proxies (El/Ca_{CaCO3}) in foraminifera (e.g., Mg/Ca as a proxy of temperature). Here we show that Na/Ca ratios in foraminifera shells could be used for reconstructing seawater Ca_{sw} concentrations in the past. Ca has a short residence time in the ocean (~1 My), whereas Na in seawater has a residence time of ~100 My. Hence it may be reasonably assumed that Na_{sw} is invariant over the Cenozoic. enabling variations in oceanic Ca to be deduced from foraminiferal Na/Ca (Na/Ca_{shell}) if Na incorporation into foraminiferal shells depends on Na/Ca in seawater. Furthermore, the paleo-concentrations of other major and minor elements may then be calculated relative to the Ca in the shells, provided that other environmental or biological factors do not present a further complication. To evaluate this hypothesis, we cultured the benthic foraminifer *Operculina ammonoides*, an extant relative of the Eocene *Nummulites*, under varying Ca_{sw} and temperature. The foraminifera grew well under the experimental conditions and increased their weight by 40-90%. The newly grown calcite (identified using a ^{135}Ba labeling in the experimental seawater) was analyzed by Laser-Ablation ICP-MS for Li, Na, Mg and Sr to Ca ratios. The relationships between Na/Ca and Mg/Ca in the shell and their ratio in the solution are best described as a power function, where the instantaneous distribution coefficient, defined here as Df, is the derivative of the power fit to the El/Ca_{shell} versus El/Ca_{sw}, In contrast, D_{Sr} and D_{Li} are invariant with El/Ca_{sw}. The influence of temperature on Li, Na and Sr incorporation was smaller than the uncertainty of our measurements. We conclude that Na/Ca in foraminiferal shells can be used to calculate paleo-calcium concentrations in the oceans and also other elements that may change relative to calcium (e.g., Mg, Sr, Li and others).

1. Introduction

1.1. Past changes in ocean chemistry

Evidence for large secular shifts in seawater chemistry are abundant throughout the geological record (e.g., Stanley and Hardie, 1998). Most of these studies have focused on oscillations in the magnesium to calcium ratio of seawater (Mg/Ca_{sw}), which indicate quasi-periodic shifts between 'calcite seas' and 'aragonite seas' (e.g., Stanley and Hardie, 1998). For this reason, it has been proposed that Mg/Ca_{sw} changes have also influenced the biomineralization and evolution of calcifying marine organisms. Mg/Ca_{sw} may also be important in determining the differential response of calcite and aragonite producing organisms to past and future climatic perturbations (Katz et al., 2010). Elemental ratios in biogenic carbonates have played a major tool in paleoceanographic research (see review in Katz et al. 2010). Mg/Ca ratio is the most studied elemental proxy and is widely utilized as a paleothermometer due to temperature dependence of Mg incorporation. However, Mg incorporation in foraminifera also depends on the seawater Mg/Ca ratio (Evans et al., 2015; Hasiuk and Lohmann, 2010; Segev and Erez, 2006), which has hampered the accuracy of these temperature reconstructions before the Pleistocene, when Mg/Ca_{sw} cannot be assumed equal to that of today (Evans et al., 2016; Lear et al., 2010). Similarly, the use of other geochemical proxies, such as Sr/Ca (e.g., Sosdian et al. 2012) and Li/Ca (Delaney and Boyle, 1986; Lear et al., 2010) is also confounded by the effects of changing seawater chemistry in general and calcium in particular, on their partitioning in biogenic carbonates. Because of the relatively short residence time of Ca in the ocean (~1 My), on time scales of few million years, variations in foraminiferal El/Ca ratios are likely driven primarily by changes in seawater Ca. However, in the longer time scales (Phanerozoic) the ratio (Mg/Ca) is influenced by changes in both elements.

Reconstruction of changes in the concentration of Ca_{sw} is also important for understanding past variability in the processes that influence the ocean calcium cycle. Calcium is delivered to the ocean predominantly by weathering and is removed mainly by burial of $CaCO_3$ on carbonate platforms and the open ocean. However, dolomitisation and the interaction of seawater with newly formed oceanic crust, also contribute to the long-term changes in seawater Mg/Ca. This implies that the concentration of these elements in seawater may be sensitive to both sea level and seafloor spreading rates (Berner, 2004). However, notwithstanding the important information derived from such seawater chemistry reconstructions, existing techniques are hampered by large uncertainties (e.g., Broecker, 2013).

Direct proxy reconstructions of Ca_{sw} are available from the modeling of fluid inclusion data in marine halite (e.g., Horita et al., 2002) and from calcium isotope measurements of carbonate oozes and marine barite (e.g., Fantle and DePaolo, 2005). Fluid inclusions are known only from a handful of time intervals (e.g., Brennan et al. 2013), but because $CaCO_3$ and gypsum are the first minerals to precipitate, the remaining solution does not contain Ca, it can only be calculated by assuming a constant relationship between Ca and SO_4 concentrations (Brennan et al., 2013; Broecker, 2013). Hence, estimates of Ca concentrations are associated with large uncertainties (Horita et al., 2002). Likewise, data from Ca isotopes are difficult to interpret given that the isotopic composition of the sources of calcium to the ocean may have changed through time and pore-water sediment interaction must be accounted for (Fantle and DePaolo, 2005). In addition, there is relatively large fractionation of Ca isotopes in biogenic carbonates (Gussone et al., 2016) which may complicate this method. As a result, there is no proxy for Ca_{sw} with an uncertainty suitable for examining the potential fine-scale changes in the calcium cycle through the Cenozoic.

Here we propose a new proxy, namely the Na/Ca ratio of foraminifera shells, as a direct method of reconstructing past changes in Ca_{sw}. Because Na has a residence time of ~100 My in seawater (Broecker et al., 1982), we hypothesize that Cenozoic variations in foraminiferal Na/Ca should principally reflect changes in Ca_{sw}. Given the abundance of dated foraminifera in sediment cores, this presents the possibility of accurately reconstructing the Ca cycle, C cycle and other seawater cations at unprecedented temporal resolution. This hypothesis cannot be tested using field calibrations because the Na/Ca_{sw} ratio in today's ocean is nearly constant. Therefore, we use culturing experiments of the benthic foraminifer *Operculina ammonoides* under a range of Ca_{sw} and temperatures with the prime goal of calibrating the potential Na/Ca proxy in foraminifera. By simultaneously measuring the Li, Mg and Sr/Ca ratios in the same specimens, we also present our findings of the response of these trace element systems to varying Ca_{sw}.

1.2. Empirical determination of distribution coefficients

Distribution coefficients of elements (DEl) that are incorporated into the lattice of inorganic and biogenic carbonates (including foraminifera) can be determined only when the experimental solutions contain different El/Ca ratios. The distribution coefficient can thus be calculated as the change in the El/Ca ratio of the $CaCO_3$ mineral versus the change in the experimental solution i.e., the slope or the derivative of the curve describing the El/Ca_{CaCO_3} versus $El/Ca_{solution}$. To achieve this goal, one needs at least three data points and an intercept that goes through zero (Figure 1A). A single point of El/Ca_{CaCO_3} divided by $El/Ca_{solution}$ should be considered as an "apparent distribution coefficient" ("DEl") and not used to describe the distribution coefficient. The regression fit of El/Ca_{CaCO_3} versus $El/Ca_{solution}$ is often not linear with a non-zero intercept (Evans et al., 2015; Hasiuk and Lohmann, 2010; Segev and Erez, 2006). We therefore propose that a proper fit that goes through the origin should be an equation of the type:

(Equation 1) $y=a \cdot x^{H}$

Where y is El/ Ca_{CaCO_3}, x is El/$Ca_{solution}$ and a and H are constants that are obtained from the power curve fit of the set of values of y versus x and cannot be obtained from a single y/x ratio (unless H=1).

This approach is following Ries (2004), Segev and Erez (2006), De Choudens-Sanchez and Gonzalez (2009) and Hasiuk and Lohmann (2010) who used it for Mg in biogenic and inorganic calcite. The theoretical basis for such relations is derived originally from Langmuir (1917) adsorption curves as modified by Freundlich (1932), providing an empirical relation between the concentration of a solute on the surface of an adsorbent to the concentration of the solute in the liquid with which it is in contact. This formulation of the equation describes integrated multi-layered adsorption as presented in Stumm and Morgan (1996, Chapter 9, Equation 14). What has often been calculated in previous studies is a linear regression of the above variables with a non-zero intercept, which is physically impossible outside of the calibrated range. Therefore, the distribution coefficient should be calculated as the derivative of the power function (Figure 1B):

(Equation 2) $D=y'=a \cdot H \cdot x^{(H-1)}$

A classic example for this behavior is the inorganic experiments of Mucci and Morse (1983) for Mg as calculated from their data by De Choudens-Sanchez and Gonzalez (2009). Note however that the latter did not calculate the derivative properly but instead have plotted the "D_{El}" (i.e., El/$Ca_{calcite}$ divided by El/$Ca_{solution}$) as the distribution coefficient, and fitted a power regression through the points. Similar approach was exercised by other authors (e.g., Evans and Müller, 2012; Hasiuk and Lohmann, 2010; Morse and Bender, 1990; Mucci and Morse, 1983; Segev and Erez, 2006). In Figure 1B we show that the distribution coefficient functions as calculated in Equation 2, does not fit the "D_{El}" both for the inorganic and

biogenic calcites (Mucci and Morse 1983 and Segev and Erez 2006, respectively). Although these previous treatments are mathematically incorrect, in most cases a serious error is unlikely to have been propagated through to fossil reconstructions as these are typically based on a calibration between an El/Ca ratio to an environmental variable (e.g., temperature).

1.3. Prior foraminiferal Na/Ca studies

Investigations of the paleoceanographic utility of Na in biogenic calcites date back several decades. Early observations of major changes in the Na content of marine carbonates have led to the suggestion that they may reflect changes in paleosalinity, an idea which was not borne out by inorganic precipitation experiments (Veizer et al., 1978). Subsequent work documented large changes in the Na composition of planktonic foraminifera throughout the Cenozoic, which were initially attributed to major changes in seawater composition (Graham et al., 1982). However, based on the distribution coefficients deduced from inorganic precipitation experiments (e.g., Kitano et al., 1975; White, 1978), it was concluded that the changes in seawater calcium required to account for the observed Na/Ca changes were too large and thus other factors might have contributed to the observed trends. These authors concluded that Na is likely to be situated in an interstitial site in the calcite lattice. However, recent studies using synchrotron X-ray spectroscopy and K-edge X-rays absorption spectral analyses, suggest that Na is structurally substituting Ca in $CaCO_3$ lattice, both in inorganic and biogenic carbonates (including foraminifera, Yoshimura et al., 2017). Early laboratory culturing work of *Trilobatus sacculifer* indicated no resolvable response of Na/Ca_{shell} to Na_{sw} at constant Ca_{sw} and no resolvable temperature dependence (Delaney et al., 1985), leading Delaney et al., (1986) to conclude that the decreasing trends in mixed planktonic Na/Ca reconstructed for the past 40 My were likely due to diagenetic recrystallization rather than changes in Ca_{sw} concentration. This interpretation was recently adopted also by Yoshimura et

al., (2017) for a 3 My record of the planktonic foraminifera *Globorotalia tumida* from the West Caroline Basin.

Other studies suggested that salinity may exert a systematic control on foraminiferal Na/Ca by the changes in activity of free Na^+, based on laboratory cultures of the benthic foraminifer *Ammonia tepida* (Wit et al., 2013). This has been tentatively confirmed in the planktonic species *G. ruber* (Allen et al., 2016), although additional effects of temperature and carbonate ion were also identified. Nonetheless, these data indicate that Na/Ca warrants further investigation as a salinity proxy and may have utility in regions where large salinity fluctuations are expected in time intervals shorter than the residence time of calcium. This salinity proxy has been field calibrated also by Mezger et al. (2016) for living *G. ruber* and *G. sacculifer* utilizing the salinity gradient of the Red Sea and compared to previous planktonic data of Delaney et al. (1985) and Allen et al. (2016).

In the present study, we investigate the factors affecting Na, Li, Mg and Sr incorporation into the shells of cultured *O. ammonoides* in a set of experiments aiming to assess the role of changes in Ca concentrations and temperature on trace element distribution functions in this important group of foraminifera (Evans et al., 2015).

2. Material and methods:

2.1. Laboratory culturing

Operculina ammonoides were collected from the North Beach, Eilat, Israel. These foraminifera are large benthic, symbiont-bearing (usually found at less than 100 m depth) and collected at a depth of ~20-25 m. Foraminifera were taken from the 475-690 μm size fraction. Live individuals were identified as those that climbed vertical glass slides placed on the sediment once returned to the laboratory.

194 In total, three sets of experiments were conducted which overlapped in scope. An initial proof
195 of concept study was followed by in-depth work examining the simultaneous effect of
196 changing Ca_{sw} and temperature, as detailed in Table 1. Prior to the experiment initiation, the
197 foraminifera were placed in seawater labeled with 40 μM Calcein for 4-5 days and only those
198 that showed fluorescent chamber were selected for the experiment. Immediately after
199 labeling, three control groups of 75 specimens each, were dried and weighed. The mean
200 weight per specimen of all control groups is 516±24 μg specimen^{-1}. The fluorescence
201 emission at 515 nm was observed using a Leica Z16 APO A MacroFluo fluorescent
202 monocular using 480 nm excitation. The detection was monitored with a Leica CCD color
203 camera DFC 310 FX.
204 For the final analysis using LA-ICP-MS (see below), we used only non-fluorescent chambers
205 following those labelled with Calcein, that grew in the experimental conditions (Figure 2). In
206 addition, the culture seawater medium was labeled with 74 nM ^{135}Ba (giving $^{135}Ba/^{138}Ba$
207 ~10× natural) in order to unambiguously identify material precipitated in culture by laser-
208 ablation, as previously described (Evans et al., 2016). No inorganic $CaCO_3$ precipitation was
209 observed in the experimental jars or on the foraminifera shells which were all inspected using
210 the fluorescent monocular.
211 The proof of concept experiment (those labeled DE2013 in Table 1) was conducted for 20
212 days and the remainder (HH2015) were conducted for 140 days. All treatments were kept
213 under a weak fluorescent light and near a window for a more natural light spectrum. The
214 overall light intensity was ~10 μmol photons m^{-2} sec^{-1}. In all cases, unfiltered Eilat seawater
215 (salinity of 40.65 psu) was used as the basis for the experimental seawaters, diluted to salinity
216 of 37 in the case of the DE2013 experiments and 35 for HH2015 using deionized water.
217 Ca_{sw} was modified by the addition of $CaCl_2$ which, given the relatively low concentration of
218 calcium in seawater, had a negligible effect on the Cl concentration. The carbonate chemistry

219 of the experimental seawaters was not modified from Gulf of Eilat seawater, except for the
220 dilution of alkalinity and DIC proportional to the salinity. Each batch of seawater was spiked
221 with the $CaCl_2$ (≥ 99.5%, Merck) to the proper concentration (Table 1) and was Immediately
222 pumped into SUPELCO gas tight bags (coated with aluminum foil) which served as
223 reservoirs for the entire experiment.
224 On commencement of the experiment, each group of foraminifera (~70 specimens) was
225 sealed in an Erlenmeyer flask (135 ml) and the water solutions were sampled and changed
226 every 1-2 weeks. The flasks were kept at constant temperature in water baths with
227 simultaneous cooling and heating. In the HH2015 experiment (representing most of the data),
228 the foraminifera were fed with different species of frozen algae after 28 days and then with
229 each change of water (Figure 3A).

230 **2.2 Analytical methods**

231 The growth rate was monitored by alkalinity depletion in each water change and weight
232 measurements of control groups at the beginning and the experimental groups at the end of
233 the experiment. Alkalinity measurements were conducted using a Radiometer TIM865
234 titration manager, with a pHC2401-8 combined pH electrode and SAC950 auto-sampler and
235 resulted in average growth of 40-90% for all treatments. At the end of the experiment, all
236 groups were washed with deionized water and treated overnight with dilute (1:10) sodium
237 hypochlorite solution (Sigma-Aldrich 10-15% analytical reagent) to remove the organic
238 matter. The use of NaOCl as an oxidative cleaning step has been previously shown not to bias
239 foraminiferal Na/Ca ratios measured by LA-ICPMS depth-profiling (supplementary material
240 of Evans et al., 2015).
241 Six specimens from each treatment were selected according to the presence of 3-13 non-
242 fluorescent chambers past the Calcein stain. These specimens were analyzed using the

RESOlution M-50 Laser Ablation system attached to an Agilent 7500ce quadropole ICPMS at Royal Holloway University of London (Evans et al., 2015). The analytical method for the determination of trace element concentrations in *O. ammonoides* is described in detail in Evans et al. (2015). Briefly, a laser spot size of 44-57 μm and repetition rate of 2 Hz was used to ablate into the marginal chord with an effective vertical spatial resolution (including cell washout time) of <1 μm. Each specimen of the six used per treatment was ablated on 4-6 chambers and each ablation spot lasted 50 seconds, which equals to 100 pulses of the laser. Therefore each experimental data point represents the mean of at least 25 laser spots (six specimens x 4-6 chambers) with the exception of DE2013 5-2 (13 laser spots) and HH2015 2B-13 (19 laser spots). Only analyses characterized by high $^{135}Ba/^{138}Ba$ ratio which was introduced to the culture seawater, were considered for this study. Since it was shown by Erez (2003) that large benthic foraminifera (e.g., *Amphistegina lobifera*) have large internal Ca pools, we verified that the newly precipitated chambers were equilibrated with the experimental seawater. The evidence for this is shown in the El/Ca ratio in the newly added chambers going from the final one backwards for the last 4-5 chambers (Figure S3). This figure shows that there is no change in any of the four elements as a function of chamber sequence (position).

Water chemistry was analyzed using Varian Vista-PRO CCD simultaneous ICP-OES at Rutgers University, USA for Na, Mg and Sr. For the Li measurements we used an Agilent 7500 ICP-MS at the Hebrew University of Jerusalem, Israel. The standard error for Li/Ca is 1.28% with the ICP-MS. For the ICP-OES, the standard errors are: Na/Ca= 1.01%, Mg/Ca= 1.02%, Sr/Ca= 0.909% calculated from the duplicates.

3. Results:

3.1. Growth

267 Based on cumulative alkalinity depletion within the experimental vessels relative to the
268 reservoirs it was possible to follow the growth of the foraminifera whilst the experiment was
269 running. In addition, as described above the weight per specimen was measured for three
270 control groups enabling total growth to be alternately estimated using the final weight of the
271 groups at the termination of the experiment after the NaOCl treatment. Total growth based on
272 the two methods was broadly similar, as shown in Figure 3B ($R^2 = 0.99$). However, mass
273 gain from alkalinity is ~20% lower than that based on weight measurements. Given that no
274 inorganic precipitation was observed at any point during the experiments in the culture
275 vessels, this probably stems from accumulation of nitrate in the vessels, perhaps due to the
276 feeding with frozen algae. The decomposition of the organic matter of these algae may
277 produce nitrate, which titrates the alkalinity. Nonetheless, in further discussions of growth,
278 we use the cumulative alkalinity data.

279 Different experiments were characterized by variable growth curves for each treatment
280 (Figure 3A). The intermediate concentrations of Ca_{sw} =12.7 and 15.3 mmol kg^{-1} showed the
281 highest $CaCO_3$ addition irrespective of temperature (Figure 3C). Calcification rates in the
282 experiment with the highest Ca (18.0 mmol kg^{-1}) were lower and approximately the same as
283 those in unmodified Gulf of Eilat seawater. Based on the mean calcification rates, it appears
284 that Ca_{sw} and not temperature is the dominant factor on growth in these experiments (Figure
285 3).

286 **3.2. Shell chemistry**

287 Seawater and foraminifera geochemical data are given in Tables 1 and 2 respectively and
288 shown in Figure 4. All the foraminiferal elemental ratios (El/Ca_{shell}) reported here vary
289 proportionally to the changes in solution Ca_{sw}, expressed hereafter as variations in element to
290 Ca ratios (El/Ca_{sw}) of the seawater media. The regression fit between the El/Ca_{shell} to El/Ca_{sw}

can be linear as seen for Sr/Ca. However, as discussed in section 1.2., in cases where the linear regression does not go through the origin (Mg/Ca and Na/Ca), a power function of the type $y=a \cdot x^H$ is more appropriate as previously suggested to account for the effect of changes in seawater Mg/Ca on its foraminiferal ratio (Hasiuk and Lohmann, 2010; Segev and Erez, 2006). Following these studies, we propose these power regressions:

(Equation 3) $Na/Ca_{shell}=2.76 \cdot 10^{-3} \cdot (Na/Ca_{sw})^{0.538}$ ($R^2 = 0.96$, Figure 4A)

(Equation 4) $Mg/Ca_{shell}=44.3 \cdot 10^{-3} \cdot (Mg/Ca_{sw})^{0.722}$ ($R^2 = 0.99$, Figure 4C)

Because shell Li and Sr/Ca varies linearly with El/Ca_{sw} and the regression approximately passes through the origin, in which case the H value of the power function is 1, we use a linear regression:

(Equation 5) $Li/Ca_{shell}=19.8 \cdot 10^{-6} \cdot (Li/Ca_{sw})$ ($R^2 = 0.94$, Figure 4B)

(Equation 6) $Sr/Ca_{shell}=0.272 \cdot 10^{-3} \cdot (Sr/Ca_{sw})$ ($R^2 = 0.98$, Figure 4D)

The experiments show no resolvable impact of temperature and growth rates on Na, Li and Sr incorporation (Figure 5). In contrast, Mg/Ca shows a strong correlation with temperature over the range that we used (22, 25, 28 ºC, Figure 5C). It is noteworthy, however, that the Mg/Ca_{shell} changes over 6 ºC temperature change, were between 12 to 17%. These changes are significantly smaller than the range of Mg/Ca changes due to the Ca manipulation (~65 %). Therefore, we used the average El/Ca_{shell} ratios of all temperature experiments for the calculations of distribution functions. We also note that during most of our experiments salinity was kept constant (at 35 and in experiment DE2013 the salinity was 37) but for all the elements the El/Ca_{shell} and the distribution function values of both data sets are coherent. In addition, we see no correlation between the elemental ratios and the calcification rates

313 which show an optimum growth at intermediate Ca concentration of 12.7 and 15.3 mmol kg^{-1}
314 (Figure 3C).

315 ## 4. Discussion

316 ### 4.1. Calcification response to varying seawater Ca and temperature

317 Previous foraminifera cultures utilizing *Heterostegina depressa* and *Ammonia tepida* have
318 shown a positive relationship between growth and Ca_{sw} (Raitzsch et al., 2010). We also
319 anticipated such response in *O. ammonoides*. However, calcification rates calculated from
320 cumulative alkalinity-depletion measurements (Figure 3C) show that at the highest Ca_{sw} the
321 calcification rates on average were the lowest of all treatments. Based on these data and also
322 that of Mewes et al. (2015), it appears that the optimum Ca_{sw} for calcification in non-
323 acclimatized foraminifera is between 13 and 15 mmol kg^{-1}. This effect is much stronger than
324 that of temperature over the range considered here. The highest Ca_{sw} (18.0 mmol kg^{-1}) may
325 have an inhibitory effect on the foraminifera and possibly on the symbiotic algae, as was
326 shown for coccolithophores (Müller et al., 2015). In addition, preliminary experiments
327 showed that at concentration of 20.3 mmol kg^{-1}, the organisms survived but did not
328 precipitate new chambers. Another possibility is that the foraminifera struggles to tightly
329 control calcification when the calcite saturation state is almost twice that compared to modern
330 seawater. For example, at least some benthic foraminifera are known to possess a carbon
331 concentrating mechanism (see the review of Erez, 2003), which means that Ω in the seawater
332 vacuoles far exceeds that of seawater. Coupled with the increased Ca_{sw} in our experiments,
333 this could lead to difficulties in suppressing spontaneous precipitation. Furthermore, given
334 that calcification is ostensibly limited by carbon rather than Ca availability (modern seawater
335 DIC/Ca = ~0.2), increasing Ca may not result in long-term calcification rate increase. Even
336 though Ca addition can enhance calcification rate, it does not facilitate enhanced carbon

transport. Regardless of the mechanism, it is clear that the observed changes in Na/Ca_{shell} cannot be attributed to changes in growth rate.

4.2. Na/Ca as a direct proxy for Ca_{sw}

In our experiments, the Na/Ca_{sw} ratio was modified by varying the Ca concentration, whilst Na was kept constant. Hence, the results demonstrate that Na/Ca_{shell} is dominantly controlled by Ca_{sw}. These results are apparently at odds with early laboratory culturing experiments of *Trilobatus sacculifer*, which suggested no resolvable response of Na/Ca_{shell} to varying Na_{sw} at constant Ca_{sw} (Delaney et al., 1985). However, the inorganic experimental data of Kitano et al. (1975), performed using solutions similar to seawater with variable Na concentrations (without Mg, resulting in calcite Na/Ca ratios similar to those of foraminifera as reported by Delaney et al. 1985), showed a clear distribution function for Na (Figure 6A).

Our Ca_{sw}-proxy calibration (Equation 3) for *O. ammonoides* offers the means to directly reconstruct Ca_{sw} over the Cenozoic using foraminifera of the family Nummulitidae. For this purpose, we use the power function (Equation 1) to obtain the concentration of Ca_{sw} using the following equation (assuming that Na is constant over the Cenozoic):

(Equation 7) $$Na/Ca_{\ shell} = a \cdot (Na/Ca_{sw})^{(H)}$$

(Equation 8) $$Ca_{sw} = \sqrt[-H]{\frac{(Na/Ca_{shell})}{a}} \cdot Na_{sw}$$

We emphasize that this equation will be accurate within the calibration range and the uncertainty will increase at lower Na/Ca_{sw}.

It has been suggested that salinity influences foraminiferal Na/Ca, probably through the control that it exerts on the activity of free Na^+ (Wit et al., 2013). Nonetheless, the sensitivity of Na/Ca_{shell} to changes in Ca_{sw} is far greater, in relative terms, than it is to salinity: The expected changes in salinity for a station in the open ocean may reach perhaps 2 psu, which

will exert a ~7% change in the Na/Ca_{shell} ratio, according to Wit et al. (2013). In our study, a change in Ca_{sw} from 10 mmol kg^{-1} (normal seawater concentration) to 18 mmol kg^{-1} exerted a change in the Na/Ca_{shell} of ~30%. The past Ca increase during the Cenozoic is estimated to have been up to three times as much (Gothmann et al., 2015), which would cause a 90% change in the Na/Ca ratio of *O. ammonoides*. Therefore, over timescales approaching the residence time of Ca_{sw}, seawater chemistry is more likely to control the Na/Ca_{shell}.

4.3. Comparison of Na incorporation into biogenic and inorganic calcite

For inorganic carbonates, relatively few experiments have focused on the incorporation of the alkali elements into calcite (Ishikawa and Ichikuni, 1984; Kitano et al., 1975; Okumura and Kitano, 1986; White, 1978), none of which were conducted using seawater solutions. Whilst Okumura and Kitano (1986) varied solution Na at constant Ca, Ishikawa and Ichikuni (1984) varied both simultaneously, demonstrating that Na/Ca in the solid is sensitive to the concentration of both, up to a $Na/Ca_{solution}$ ratio of ~200 mol mol^{-1}, approximately four times that of present-day seawater. Coupled with the observation that the degree of alkali element incorporation depends on ionic radius, White (1978) and Okumura and Kitano (1986) concluded that Na is likely to be situated in an interstitial site in the calcite lattice. However, Yoshimura et al. (2017) concluded, according to synchrotron X-ray spectroscopy and K-edge X-rays absorption spectral analyses, that Na is structurally substituting Ca in $CaCO_3$ lattice, both in inorganic and biogenic carbonates (including foraminifera). In addition, they proposed that the mechanism for charge compensation is through the creation of CO_3^{2-} vacancies. Either way, these inorganic precipitation experiments and observations form an empirical basis for the use of Na/Ca in foraminiferal calcite as a potential proxy of solution Na/Ca. Hence we may expect Na/Ca_{sw} to exert a primary influence on foraminiferal Na/Ca, particularly since it has been demonstrated that seawater is present at the site of

385 biomineralization (Bentov et al., 2009; Erez, 2003) and that *O. ammonoides* is well labeled
386 by the cell impermeable dye Calcein (Figure 2). Although it has been suggested that some
387 foraminifera facilitate calcification by transporting Ca to the site of biomineralization
388 (Nehrke et al., 2013), which would also lower the Na/Ca ratio, this cannot be the case for *O.*
389 *ammonoides* as the Nummulitid foraminifera are characterized by a Mg/Ca ratio similar to
390 inorganic calcite. If significant Ca transport took place, then this would reduce the shell
391 Mg/Ca and Na/Ca ratio relative to inorganic calcite precipitated from seawater, yet this is not
392 the case (Figure 6C). Further discussion of this subject is given in Evans et al. (2018).

393 ### 4.4. Insights into the incorporation of Mg, Li and Sr

394 Mg/Ca is the only ratio reported here with a direct response to temperature (Figure 5), as
395 previously shown for other benthic species including *O. ammonoides* (see the review of Katz
396 et al., 2010). The data here broadly conform to previous work with high-Mg *Rotaliid*
397 foraminifera, being characterized by a Mg/Ca-temperature sensitivity approximately three
398 times lower than low-Mg planktonic species. In the present study, averaging the data from all
399 experiments defines a 2.60 mmol mol^{-1} increase in Mg/Ca_{shell} per °C, in good agreement with
400 that for the same species in unmodified seawater (2.57 mmol mol^{-1} $°C^{-1}$, see Evans et al.,
401 2015). This result indicates that the sensitivity of Mg/Ca to temperature in high-Mg benthic
402 species does not vary as a function of Ca_{sw}. Similarly, the nonlinear response of Mg/Ca_{shell} to
403 Mg/Ca_{sw} (Figure 4) is in good agreement with *O. ammonoides* cultures under variable Mg_{sw}.
404 Furthermore, as originally shown by Segev and Erez (2006), Mg/Ca_{shell} in the benthic
405 foraminifera *Amphistegina* also responded non-linearly to Mg/Ca_{sw}, rather than the
406 concentration of Mg or Ca.
407

Li/Ca in *O. ammonoides* has been previously shown to be sensitive to Li_{sw} with a linear distribution function (Evans et al., 2015). Here, we find that Li/Ca_{shell} is also sensitive to Ca_{sw} at constant Li with a constant D_{Li} (Figure 4B). The clear influence of Ca_{sw} on the Li/Ca_{shell} is at odds with recent investigations using *Amphistegina lessonii* (Langer et al., 2015) suggestion that D_{Li} should be expressed relative to Li_{sw} rather than Li/Ca_{sw} and is manifestly not supported by our work. Furthermore, Langer et al. (2015) present two sets of cultures wherein Li_{sw} and Ca_{sw} were varied independently, yet where these overlap close to the natural Li/Ca_{sw} ratio there is a factor of two difference in the measured foraminifera Li/Ca ratios, potentially pointing to a complication with that experiment. Moreover, our results indicate that Li incorporation is entirely consistent with ion transport dominantly through seawater vacuolization, i.e., Li/Ca_{shell} is dominantly controlled by Li/Ca_{sw} irrespective of whether Li_{sw} or Ca_{sw} is varied.

Strontium in *O. ammonoides* also show a linear distribution function over the range measured in our experiment (Figure 4D). In common with Li, but unlike the other trace elements in this study, the exponent (H) is equal to 1 so that a linear fit goes through the origin (Figure 4D). Based on previous studies Sr in calcite is known to be dependent on calcite Mg/Ca, which in turn is principally dependent on Mg/Ca_{sw}, probably because Mg-induced lattice distortion modifies the ease with which Sr may substitute for Ca (Mucci and Morse, 1983). This was also demonstrated to be the case for foraminifera (Evans et al. 2015). Therefore, we stress that the D_{Sr} defined in Equation 6 is relevant in situations where Sr/Ca_{sw} and Mg/Ca_{sw} vary proportionally to each other (as is the case here). When Sr/Ca_{sw} varies through changing Sr_{sw}, D_{Sr} is higher because Mg/Ca_{shell} is constant (Evans et al. 2015). Examining this change in the context of both inorganic calcite precipitated from seawater and *O. ammonoides* cultured

under variable Sr_{sw} shows that the sensitivity of D_{Sr} to $Mg/Ca_{calcite}$ is equivalent irrespective of how the calcite Mg/Ca ratio is modified.

Our *O. ammonoides* culture data are shown in the context of a compilation of data from the literature on both foraminiferal and inorganic calcite in Figure 6 (Bender et al., 1975; De Choudens-Sanchez and Gonzalez, 2009; Delaney et al., 1985; Delaney and Boyle, 1986; Dissard et al., 2010; Evans et al., 2016, 2015; Hall and Chan, 2004; Hathorne and James, 2006; Kitano et al., 1975; Lea et al., 1999; Mucci and Morse, 1983; Raitzsch et al., 2010; Segev and Erez, 2006; Vigier et al., 2015; Wit et al., 2013), and the derivative of the power functions, i.e., the distribution functions, are shown in Figure 7. This highlights the widely different trace element concentrations between groups of foraminiferal species with differing Mg/Ca ratios. These groups are presented in Figure 6 as high-Mg (> 8 $\%MgCO_3$), intermediate-Mg (3-8 $\%MgCO_3$) and low-Mg (< 3 $\%MgCO_3$) foraminifera (Bentov and Erez, 2006). This data compilation also contains core top samples with the present day's ocean El/Ca ratios, which fit well on the experimental regression lines. An interesting pattern emerges from Figure 6: Whereas each element has a distribution function of the type shown in Equation 1, the actual concentrations of each element in the calcite (foraminifera and inorganic) show strong correspondence to the Mg content. Whilst this was already discussed for Sr, we note that a similar explanation may also be given for Na and Li. Particularly, this has been previously argued for the incorporation of Na into both inorganic and foraminiferal calcite (Bender et al., 1975; Evans et al., 2015; Graham et al., 1982; Okumura and Kitano, 1986; Yoshimura et al., 2017). Therefore, the effect of Mg should be accounted for when applying our calibration to different foraminifera species in the paleo records, as changing Ca_{sw} also exerts direct control on $Mg/Ca_{calcite}$. Indeed, this dependency of Na on Mg content in the shell is well displayed in Figure 6, where high-Mg *O. ammonoides* show much higher

457 Na/Ca then low-Mg species. Similarly, Okumura and Kitano (1986) precipitated $CaCO_3$ from
458 solutions both with and without the addition of $MgCl_2$ and demonstrated that compared to
459 solution without Mg the presence of ~50 mmol kg^{-1} Mg doubles the concentration of Na in
460 calcite at a given solution Na/Ca ratio. We also note that similar relations between Mg and
461 other trace elements are found within shells of individual foraminifera displaying alternations
462 of Mg-rich and Mg-poor layers (e.g., Bentov and Erez, 2006).

463 5. **Conclusions**

464 In this study we cultured the benthic foraminifer *Operculina ammonoides* under variable
465 seawater Ca concentrations (Ca_{sw}). These laboratory experiments demonstrate that Na
466 incorporation into their calcitic shells is principally related to the seawater Na/Ca ratio, with
467 no resolvable temperature sensitivity. Given the long residence time of Na in seawater (~100
468 My) as opposed to that of Ca_{sw} (1 My), our calibration provides a detailed empirical basis for
469 the use of foraminiferal Na/Ca as a direct method of reconstructing Ca_{sw}. We further
470 demonstrate that the determination of the distribution functions cannot be obtained with a
471 single El/Ca_{shell} divided by El/Ca_{sw}. Instead, the El/Ca in the experimental solution needs to
472 be varied in order to constrain the power function that appropriately describes the distribution
473 function for each element (Na included), as recently shown for D_{Mg}. Perhaps a new notation
474 should be introduced to describe the distribution function: Df_{El} (e.g., Df_{Na}).
475 Whilst the data presented here are derived from *O. ammonoides*, it has been shown that
476 calibrations based on this foraminifer are applicable to the abundant Eocene *Nummulites*
477 (Evans et al. 2013). Future similar experiments in other benthic and planktonic foraminifera
478 would be needed to accurately determine species-specific distribution functions that will
479 allow for future reconstructions of Ca_{sw} concentrations in the past. We note, however, that as
480 for any other geochemical system, further investigations of the influence secondary effects,
481 such as variations in Mg/Ca, salinity and diagenetic alteration are needed to improve the

accuracy of this proxy. Nonetheless, at least for *O. ammonoides*, the changes in Ca_{sw} are likely the dominant control on the shell's Na/Ca.

Finally, we examine the response of shell Li, Mg and Sr under variable Ca_{sw} and find that these elements are sensitive to this change, in contrast to some previous work on benthic foraminifera. The Sr distribution function is modified by calcite Mg/Ca, as previously demonstrated for this species and inorganic calcite. Together, a better understanding of the incorporation of these other trace elements means that Na/Ca may be coupled with Li, Mg and Sr in order to simultaneously reconstruct the history of a range of seawater cations and therefore the processes controlling their cycling in seawater to be unraveled.

Acknowledgements

This study is funded by NSF-BSF project 1634573 and by ISF project 790/16.

Thanks to Shai Oron, Oriya Moav and Tanya Rivlin from the marine laboratory in Eilat for the help with collecting the foraminifera.

References:

Allen, K.A., Hönisch, B., Eggins, S.M., Haynes, L.L., Rosenthal, Y., Yu, J., 2016. Trace element proxies for surface ocean conditions: A synthesis of culture calibrations with planktic foraminifera. Geochim. Cosmochim. Acta 193, 197–221. doi:10.1016/j.gca.2016.08.015

Bender, M.L., Lorens, R.B., Williams, D.F., 1975. Sodium, magnesium and strontium in the test of planktonic foraminifera. Micropaleontology 21, 448–459. doi:10.2307/1485293

Bentov, S., Brownlee, C., Erez, J., 2009. The role of seawater endocytosis in the biomineralization process in calcareous foraminifera. Proc. Natl. Acad. Sci. U. S. A. 106, 21500–21504. doi:10.1073/pnas.0906636106

Bentov, S., Erez, J., 2006. Impact of biomineralization processes on the Mg content of foraminiferal shells: A biological perspective. Geochemistry, Geophys. Geosystems 7. doi:10.1029/2005GC001015

Berner, R.A., 2004. A model for calcium , magnesium and sulfate in seawater over

511 Phanerozoic time. Am. J. Sci. 304, 438–453.
512 Brennan, S.T., Lowenstein, T.K., Cendon, D.I., 2013. The major-ion composition of cenozoic
513 seawater: the past 36 million years from fluid inclusions inmarine halite. Am. J. Sci.
514 313, 713–775. doi:10.2475/08.2013.01
515 Broecker, W., 2013. How to think about the evolution of the ratio of Mg to Ca in seawater.
516 Am. J. Sci. 313, 776–789. doi:10.2475/08.2013.02
517 Broecker, W.S., Peng, T.H., Beng, Z., 1982. Tracers in the sea, Lamont-Doherty Geologica.
518 doi:10.1016/0016-7037(83)90075-3
519 De Choudens-Sanchez, V., Gonzalez, L.A., 2009. Calcite and Aragonite Precipitation Under
520 Controlled Instantaneous Supersaturation: Elucidating the Role of CaCO3 Saturation
521 State and Mg/Ca Ratio on Calcium Carbonate Polymorphism. J. Sediment. Res. 79,
522 363–376. doi:10.2110/jsr.2009.043
523 Delaney, M.L., Bé, A., Boyle, E.A., 1985. Li, Sr, Mg, and Na in foraminiferal calcite shells
524 from laboratory culture, sediment traps, and sediment cores. Geochim. Cosmochim.
525 Acta 49, 1327–1341. doi:10.1016/0016-7037(85)90284-4
526 Delaney, M.L., Boyle, E.A., 1986. Lithium in foraminiferal shells: implications for high-
527 temperature hydrothermal circulation fluxes and oceanic crustal generation rates. Earth
528 Planet. Sci. Lett. 80, 91–105. doi:10.1016/0012-821X(86)90022-1
529 Dissard, D., Nehrke, G., Reichart, G.J., Bijma, J., 2010. The impact of salinity on the Mg/Ca
530 and Sr/Ca ratio in the benthic foraminifera Ammonia tepida: Results from culture
531 experiments. Geochim. Cosmochim. Acta 74, 928–940. doi:10.1016/j.gca.2009.10.040
532 Erez, J., 2003. The source of ions for biomineralization in foraminifera and their implications
533 for paleoceanographic proxies (Review). Rev. Mineral. geochemistry 54, 115.
534 doi:10.2113/0540115
535 Evans, D., Brierley, C., Raymo, M.E., Erez, J., Müller, W., 2016. Planktic foraminifera shell
536 chemistry response to seawater chemistry: Pliocene-Pleistocene seawater Mg/Ca,
537 temperature and sea level change. Earth Planet. Sci. Lett. 438, 139–148.
538 doi:10.1016/j.epsl.2016.01.013
539 Evans, D., Erez, J., Oron, S., Müller, W., 2015. Mg/Ca-temperature and seawater-test
540 chemistry relationships in the shallow-dwelling large benthic foraminifera Operculina
541 ammonoides. Geochim. Cosmochim. Acta 148, 325–342. doi:10.1016/j.gca.2014.09.039
542 Evans, D., Müller, W., 2012. Deep time foraminifera Mg/Ca paleothermometry: Nonlinear
543 correction for secular change in seawater Mg/Ca. Paleoceanography 27, 1–11.
544 doi:10.1029/2012PA002315

Evans, D., Müller, W., Erez, J., 2018. Assessing foraminifera biomineralisation models through trace element data of cultures under variable seawater chemistry. Geochim. Cosmochim. Acta. doi:10.1016/J.GCA.2018.02.048

Fantle, M.S., DePaolo, D.J., 2005. Variations in the marine Ca cycle over the past 20 million years. Earth Planet. Sci. Lett. 237, 102–117. doi:10.1016/j.epsl.2005.06.024

Freundlich, H., 1932. Of the adsorption of gases. Section II. Kinetics and energetics of gas adsorption. Trans. Faraday Soc. 28, 195–201. doi:10.1039/TF9322800195

Gothmann, A.M., Stolarski, J., Adkins, J.F., Schoene, B., Dennis, K.J., Schrag, D.P., Mazur, M., Bender, M.L., 2015. Fossil corals as an archive of secular variations in seawater chemistry since the Mesozoic. Geochim. Cosmochim. Acta 160, 188–208. doi:10.1016/j.gca.2015.03.018

Graham, D.W., Bender, M.L., Williams, D.F., Keigwin, L.D., 1982. Strontium-calcium ratios in Cenozoic planktonic foraminifera. Geochim. Cosmochim. Acta 46, 1281–1292. doi:10.1016/0016-7037(82)90012-6

Gussone, N., Schmitt, A.-D., Heuser, A., Wombacher, F., Dietzel, M., Tipper, E., Schiller, M., 2016. Calcium Stable Isotope Geochemistry, 1st ed. Springer Berlin Heidelberg, Berlin. doi:10.1007/978-3-540-68953-9_6

Hall, J.M., Chan, L.H., 2004. Li/Ca in multiple species of benthic and planktonic foraminifera: Thermocline, latitudinal, and glacial-interglacial variation. Geochim. Cosmochim. Acta 68, 529–545. doi:10.1016/S0016-7037(00)00451-4

Hasiuk, F.J., Lohmann, K.C., 2010. Application of calcite Mg partitioning functions to the reconstruction of paleocean Mg/Ca. Geochim. Cosmochim. Acta 74, 6751–6763. doi:10.1016/j.gca.2010.07.030

Hathorne, E.C., James, R.H., 2006. Temporal record of lithium in seawater: A tracer for silicate weathering? Earth Planet. Sci. Lett. 246, 393–406. doi:10.1016/j.epsl.2006.04.020

Horita, J., Zimmermann, H., Holland, H.D., 2002. Chemical evolution of seawater during the Phanerozoic: Implications from the record of marine evaporites. Geochim. Cosmochim. Acta 66, 3733–3756. doi:10.1016/S0016-7037(01)00884-5

Ishikawa, M., Ichikuni, M., 1984. Uptake of sodium and potassium by calcite. Chem. Geol. 42, 137–146. doi:10.1016/0009-2541(84)90010-X

Katz, M.E., Cramer, B.S., Franzese, a., Honisch, B., Miller, K.G., Rosenthal, Y., Wright, J.D., 2010. Traditional and Emerging Geochemical Proxies in Foraminifera. J. Foraminifer. Res. 40, 165–192. doi:10.2113/gsjfr.40.2.165

579 Kitano, Y., Okumura, M., Idogaki, M., 1975. Incorporation of sodium, chloride and sulfate
580 with calcium carbonate. Geochem. J. 9, 75–84. doi:10.2343/geochemj.9.75
581 Langer, G., Sadekov, A., Thoms, S., Mewes, A., Nehrke, G., Greaves, M., Misra, S., Bijma,
582 J., Elderfield, H., 2015. Li partitioning in the benthic foraminifera Amphistegina
583 lessonii. Geochemistry Geophys. Geosystems 16, 4275–4279.
584 doi:10.1002/2014GC005684.Key
585 Langmuir, I., 1917. The constitution and fundamental properties of solids and liquids. II.
586 Liquids. J. Am. Chem. Soc. 39, 1848–1906. doi:10.1021/ja02254a006
587 Lea, D.W., Mashiotta, T. a., Spero, H.J., 1999. Controls on magnesium and strontium uptake
588 in planktonic foraminifera determined by live culturing. Geochim. Cosmochim. Acta 63,
589 2369–2379. doi:10.1016/S0016-7037(99)00197-0
590 Lear, C.H., Mawbey, E.M., Rosenthal, Y., 2010. Cenozoic benthic foraminiferal Mg/Ca and
591 Li/Ca records: Toward unlocking temperatures and saturation states. Paleoceanography
592 25, 1–11. doi:10.1029/2009PA001880
593 Mewes, A., Langer, G., Thoms, S., Nehrke, G., Reichart, G.-J., de Nooijer, L.J., Bijma, J.,
594 2015. Impact of seawater [Ca2+] on the calcification and calcite Mg / Ca of
595 Amphistegina lessonii. Biogeosciences 12, 2153–2162. doi:10.5194/bg-12-2153-2015
596 Mezger, E.M., de Nooijer, L.J., Boer, W., Brummer, G.J.A., Reichart, G.J., 2016. Salinity
597 controls on Na incorporation in Red Sea planktonic foraminifera. Paleoceanography 31,
598 1562–1582. doi:10.1002/2016PA003052
599 Morse, J.W., Bender, M.L., 1990. Partition coefficients in calcite: Examination of factors
600 influencing the validity of experimental results and their application to natural systems.
601 Chem. Geol. 82, 265–277. doi:10.1016/0009-2541(90)90085-L
602 Mucci, A., Morse, J.W., 1983. The incorporation of Mg2+ and Sr2+ into calcite overgrowths:
603 influences of growth rate and solution composition. Geochim. Cosmochim. Acta 47,
604 217–233. doi:http://dx.doi.org/10.1016/0016-7037(83)90135-7
605 Müller, M.N., Barcelos E Ramos, J., Schulz, K.G., Riebesell, U., Kaźmierczak, J., Gallo, F.,
606 Mackinder, L., Li, Y., Nesterenko, P.N., Trull, T.W., Hallegraeff, G.M., 2015.
607 Phytoplankton calcification as an effective mechanism to alleviate cellular calcium
608 poisoning. Biogeosciences 12, 6493–6501. doi:10.5194/bg-12-6493-2015
609 Nehrke, G., Keul, N., Langer, G., De Nooijer, L.J., Bijma, J., Meibom, A., 2013. A new
610 model for biomineralization and trace-element signatures of Foraminifera tests.
611 Biogeosciences 10, 6759–6767. doi:10.5194/bg-10-6759-2013
612 Okumura, M., Kitano, Y., 1986. Coprecipitation of alkali metal ions with calcium carbonate.

613 Geochim. Cosmochim. Acta 50, 49–58. doi:10.1016/0016-7037(86)90047-5
614 Raitzsch, M., Dueñas-Bohórquez, A., Reichart, G.-J., de Nooijer, L.J., Bickert, T., 2010.
615 Incorporation of Mg and Sr in calcite of cultured benthic foraminifera: impact of
616 calcium concentration and associated calcite saturation state. Biogeosciences 7, 869–
617 881. doi:10.5194/bg-7-869-2010
618 Ries, J.B., 2004. Effect of ambient Mg/Ca ratio on Mg fractionation in calcareous marine
619 invertebrates: A record of the oceanic Mg/Ca ratio over the Phanerozoic. Geology 32,
620 981–984. doi:10.1130/G20851.1
621 Segev, E., Erez, J., 2006. Effect of Mg/Ca ratio in seawater on shell composition in shallow
622 benthic foraminifera. Geochemistry, Geophys. Geosystems 7, 1–8.
623 doi:10.1029/2005GC000969
624 Sosdian, S.M., Lear, C.H., Tao, K., Grossman, E.L., O'Dea, A., Rosenthal, Y., 2012.
625 Cenozoic seawater Sr/Ca evolution. Geochemistry, Geophys. Geosystems 13, 1–23.
626 doi:10.1029/2012GC004240
627 Stanley, S.M., Hardie, L.A., 1998. Secular oscillations in the carbonate mineralogy of reef-
628 building and sediment-producing organisms driven by tectonically forced shifts in
629 seawater chemistry. Palaeogeogr. Palaeoclimatol. Palaeoecol. 144, 3–19.
630 doi:10.1016/S0031-0182(98)00109-6
631 Stumm, W., Morgan, J.J., 1996. Aquatic Chemistry: Chemical Equilibria and Rates in
632 Natural Waters, 3rd ed. Wiley.
633 Veizer, J., Lemieux, J., Jones, B., Gibling, M.R., Savelle, J., 1978. Paleosalinity and
634 dolomitization of a Lower Paleozoic carbonate sequence, Somerset and Prince of Wales
635 Islands, Arctic Canada. Can. J. Earth Sci. 15, 1448–1461. doi:10.1139/e78-151
636 Vigier, N., Rollion-Bard, C., Levenson, Y., Erez, J., 2015. Lithium isotopes in foraminifera
637 shells as a novel proxy for the ocean dissolved inorganic carbon (DIC). Comptes Rendus
638 - Geosci. 347, 43–51. doi:10.1016/j.crte.2014.12.001
639 White, A.F., 1978. Sodium coprecipitation in calcite and dolomite. Chem. Geol. 23, 65–72.
640 doi:10.1016/0009-2541(78)90065-7
641 Wit, J.C., de Nooijer, L.J., Wolthers, M., Reichart, G.J., 2013. A novel salinity proxy based
642 on Na incorporation into foraminiferal calcite. Biogeosciences 10, 6375–6387.
643 doi:10.5194/bg-10-6375-2013
644 Yoshimura, T., Tamenori, Y., Suzuki, A., Kawahata, H., Iwasaki, N., Hasegawa, H., Nguyen,
645 L.T., Kuroyanagi, A., Yamazaki, T., Kuroda, J., Ohkouchi, N., 2017. Altervalent
646 substitution of sodium for calcium in biogenic calcite and aragonite. Geochim.

647 Cosmochim. Acta 202, 21–38. doi:10.1016/j.gca.2016.12.003
648

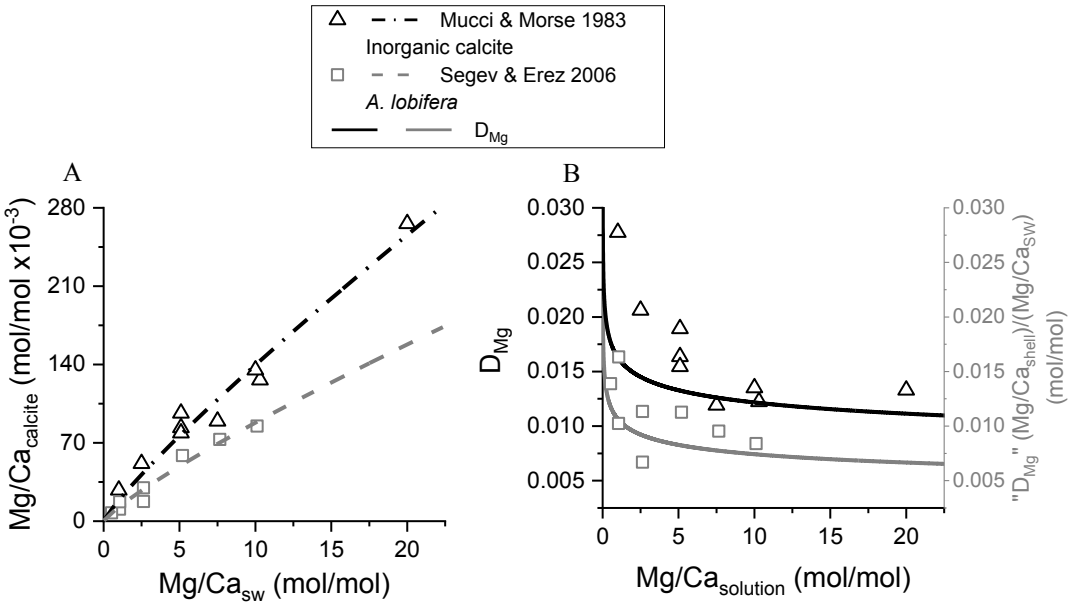

Fig. 1: Calculations of distribution functions for Mg in calcite precipitated from seawater for inorganic (black) and foraminiferal (grey) experimental data (Mucci & Morse, 1983 and Segev & Erez, 2006, respectively). **(A)** Power fit through the data for the inorganic experiment: $Mg/Ca_{calcite}=18.7 \times (Mg/Ca_{solution})^{0.87}$, $R^2=0.96$, and for the biogenic data $Mg/Ca_{calcite}=12.6 \times (Mg/Ca_{solution})^{0.84}$, $R^2=0.96$. **(B)** Magnesium distribution functions calculated as the derivative of the power fit (solid lines) from figure A. The symbols represent the "apparent distribution coefficients" ("D_{Mg}"), calculated from the individual data points. Despite the similar behavior (i.e., increase in lower $Mg/Ca_{solution}$) there are considerable differences between the derivatives (the distribution functions) and the "apparent distribution coefficients" ("D_{Mg}"). For the inorganic derivative: $D_{Mg}=16.3 \times 10^{-3} \times (Mg/Ca_{solution})^{-0.13}$ and for the biogenic $D_{Mg}=10.7 \times 10^{-3} \times (Mg/Ca_{solution})^{-0.16}$.

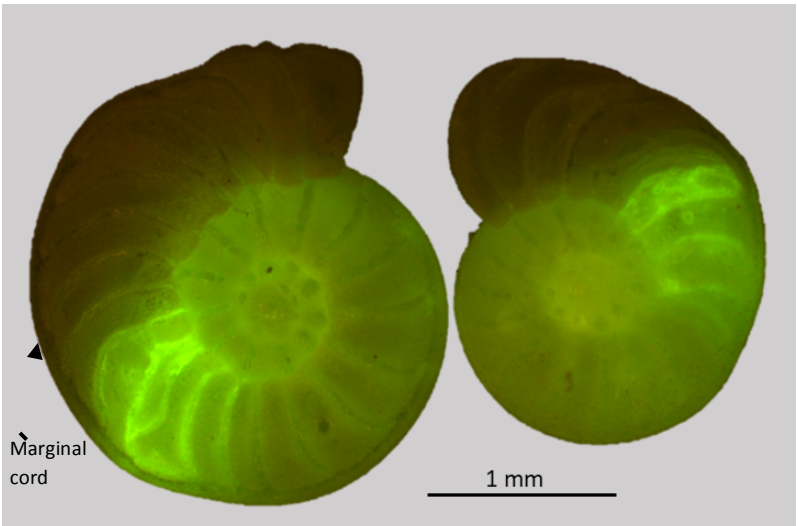

Figure 2: Example of specimens of *O. ammonoides* used in this experiment: the organisms were incubated with the fluorescent dye Calcein which mark the chambers precipitated prior to the experiment. The dark, non-fluorescent chambers consist of newly precipitated $CaCO_3$ during the experimental conditions which were selected for analysis. The laser spots were

with a diameter of 44 µm were made on the marginal cord (shown by black arrow) on 4-6 chambers per specimen (a total of ~25 analyses per treatment).

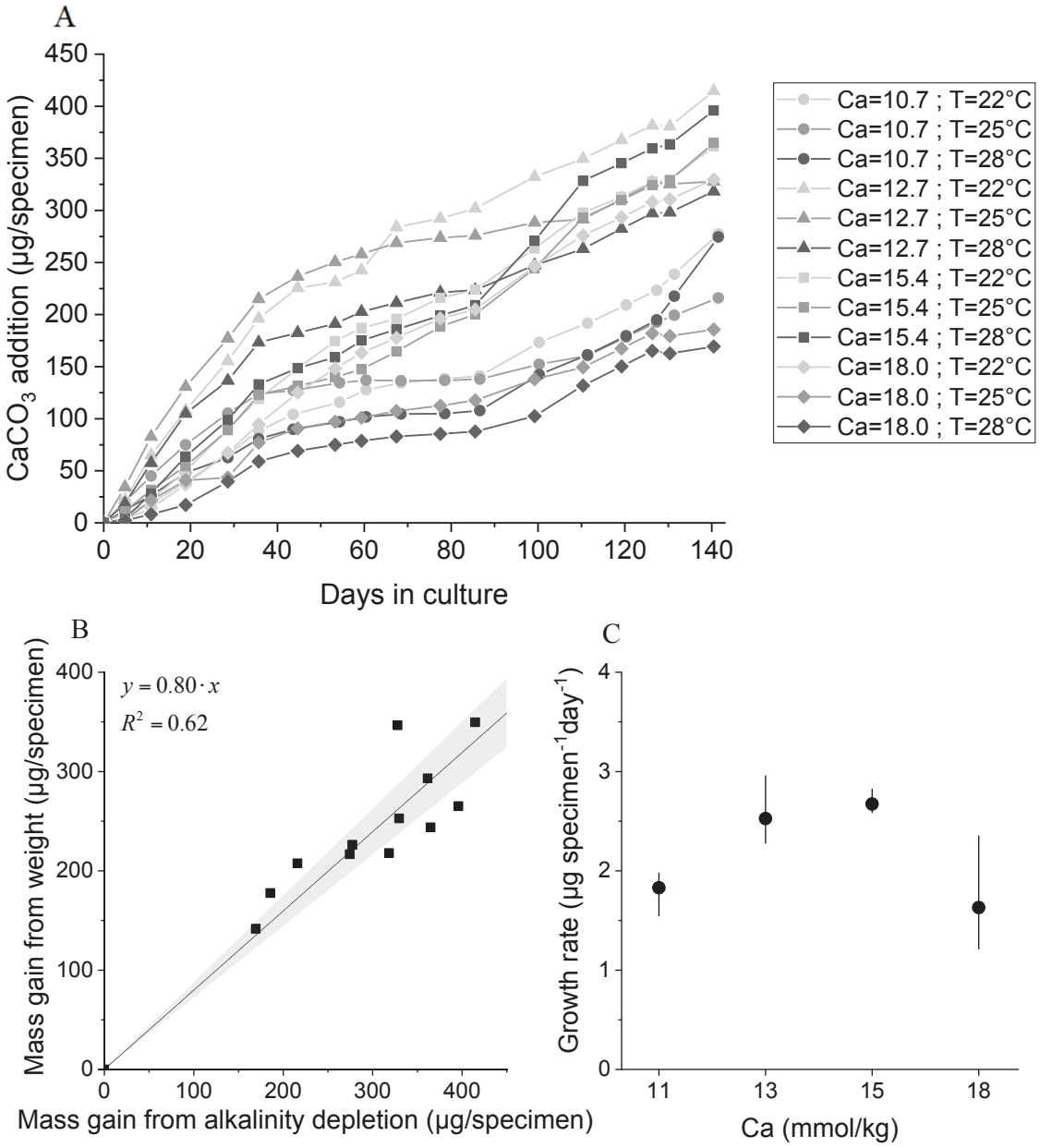

Figure 3: Growth of the foraminifera during the experiment **(A)** Cumulative $CaCO_3$ addition for each treatment versus time, calculated from alkalinity depletion measurements. Different symbols represent seawater Ca concentrations (in mmol kg^{-1}), whilst different shades of grey represent different temperatures. **(B)** Weight increase per specimen relative to their initial weight (from control groups) compared to the alkalinity depletion (see discussion for the difference). **(C)** Mean growth rates per specimen as a function of Ca_{sw}. The symbols are the average for each Ca_{sw} concentration and the vertical bars show the range for the three temperatures. A clear optimum is observed between 13 and 15 mmol kg^{-1}.

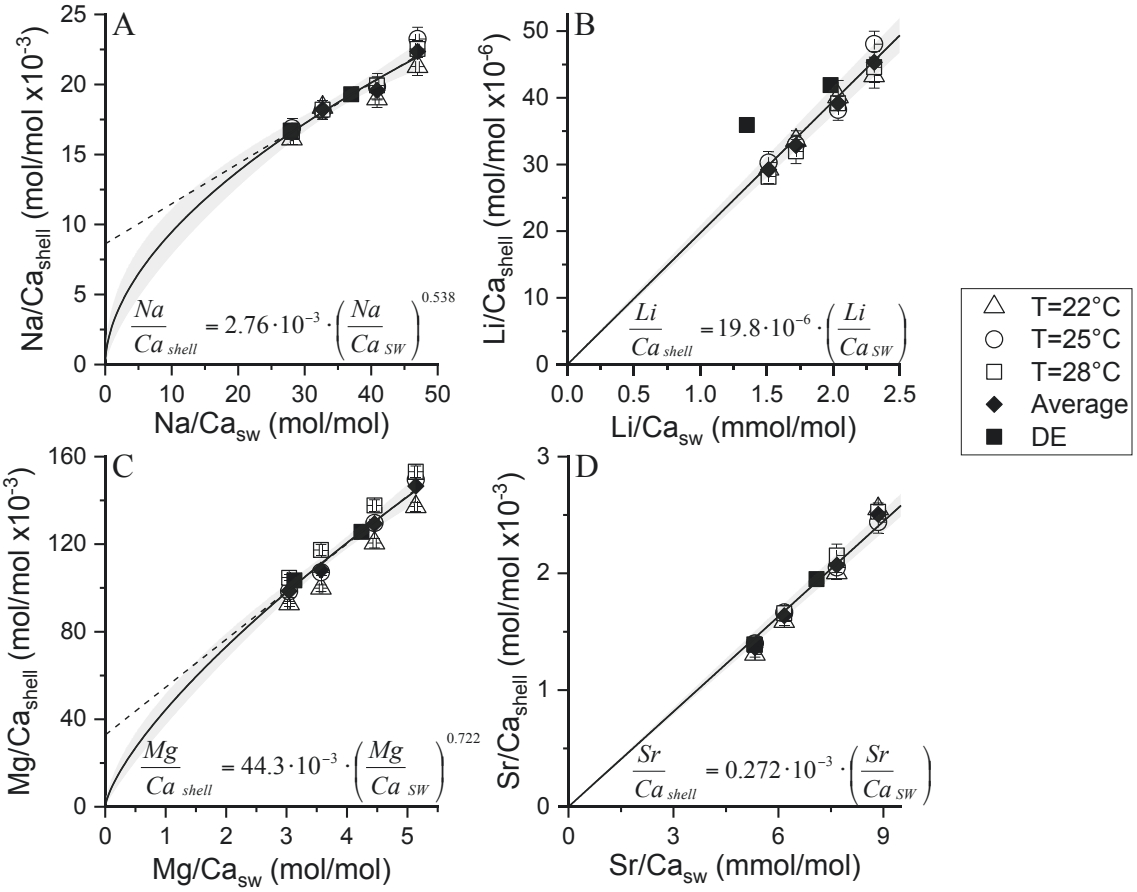

Figure 4: Foraminifera El/Ca data as a function of the respective El/Ca ratio in the experimental seawater (see Table 1 and 2 for details). Linear regressions for Na (A) and Mg (C) have a non-zero intercept with the Y axis and therefore we use power fit that goes through the origin (see full explanation in section 1.2). For Li (B) and Sr (D) the distribution coefficients are constant. For the Li fit, we excluded the one outlying data point of the proof of concept experiment (DE in Tables 1 and 2). The shaded area is the 95% confidence bands.

El/Ca	*Power fit (·10^{-3})*	R^2	*Linear fit (·10^{-3})*	R^2
Na/Ca	$Na/Ca_{shell} = 2.76 \times (Na/Ca_{sw})^{0.538}$	0.964	$Na/Ca_{shell} = 0.283 \times (Na/Ca_{sw}) + 8.73$	0.969
Mg/Ca	$Mg/Ca_{shell} = 44.3 \times (Mg/Ca_{sw})^{0.722}$	0.986	$Mg/Ca_{shell} = 21.9 \times (Mg/Ca_{sw}) + 32.8$	0.988
Li/Ca	$Li/Ca_{shell} = 19.0 \cdot 10^{-3} \times (Li/Ca_{sw})^{1.056}$	0.941	$Li/Ca_{shell} = 19.8 \cdot 10^{-3} \times (Li/Ca_{sw})$	0.939
Sr/Ca	$Sr/Ca_{shell} = 0.189 \times (Sr/Ca_{sw})^{1.19}$	0.997	$Sr/Ca_{shell} = 0.272 \times (Sr/Ca_{sw})$	0.977

Given that in our experiments we only changed the seawater Ca concentrations whereas Na concentration remained constant (considering its long oceanic residence time of ~100 My), we can also express the foraminiferal Na/Ca as a function of seawater Ca. It is noteworthy, however, that these equations are only applicable within the calibration range.

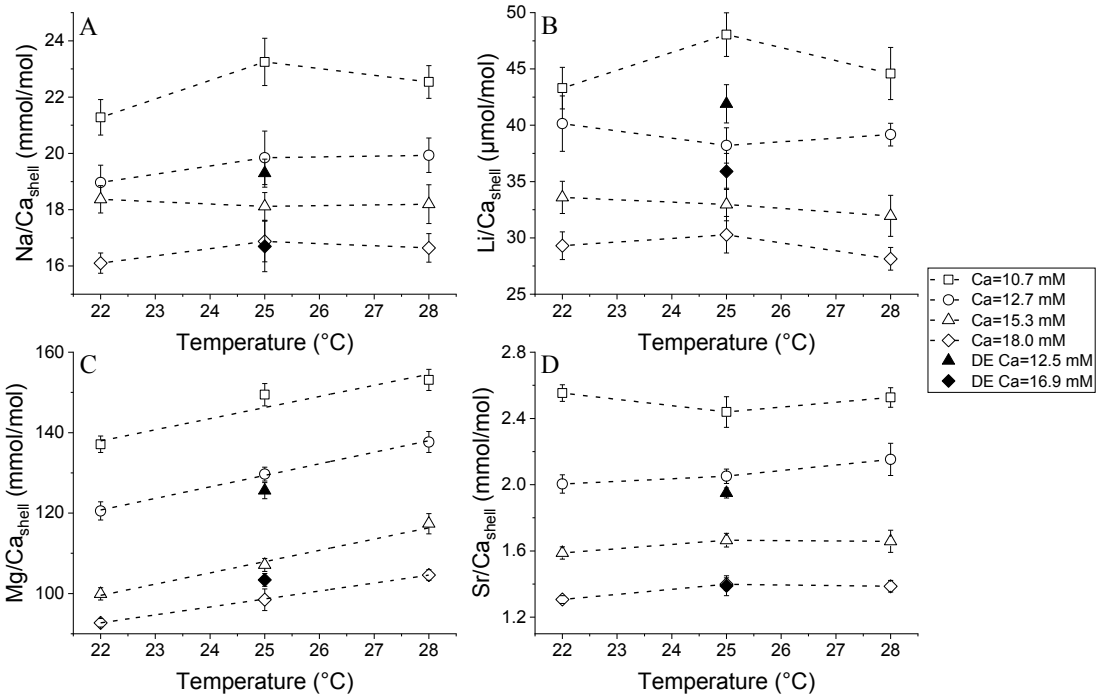

Figure 5: The effect of temperature on the Ca experiments: for Na Li and Sr, there is no visible temperature effect (A, B, D), whilst Mg shows a clear increase with temperature at each Ca concentration. **(C)** The linear correlations of Mg with temperature are: Ca=10.7 mmol kg^{-1}: Mg/Ca$_{shell}$=2.76 x Temp+77.2, R^2=0.93; Ca=12.7 mmol kg^{-1}: Mg/Ca$_{shell}$=2.87 x Temp+57.7, R^2=0.998; Ca=15.3 mmol kg^{-1}: Mg/Ca$_{shell}$=2.80 x Temp+37.9, R^2=0.99; Ca=18.0 mmol kg^{-1}: Mg/Ca$_{shell}$=1.98 x Temp+49.2, R^2=0.999.

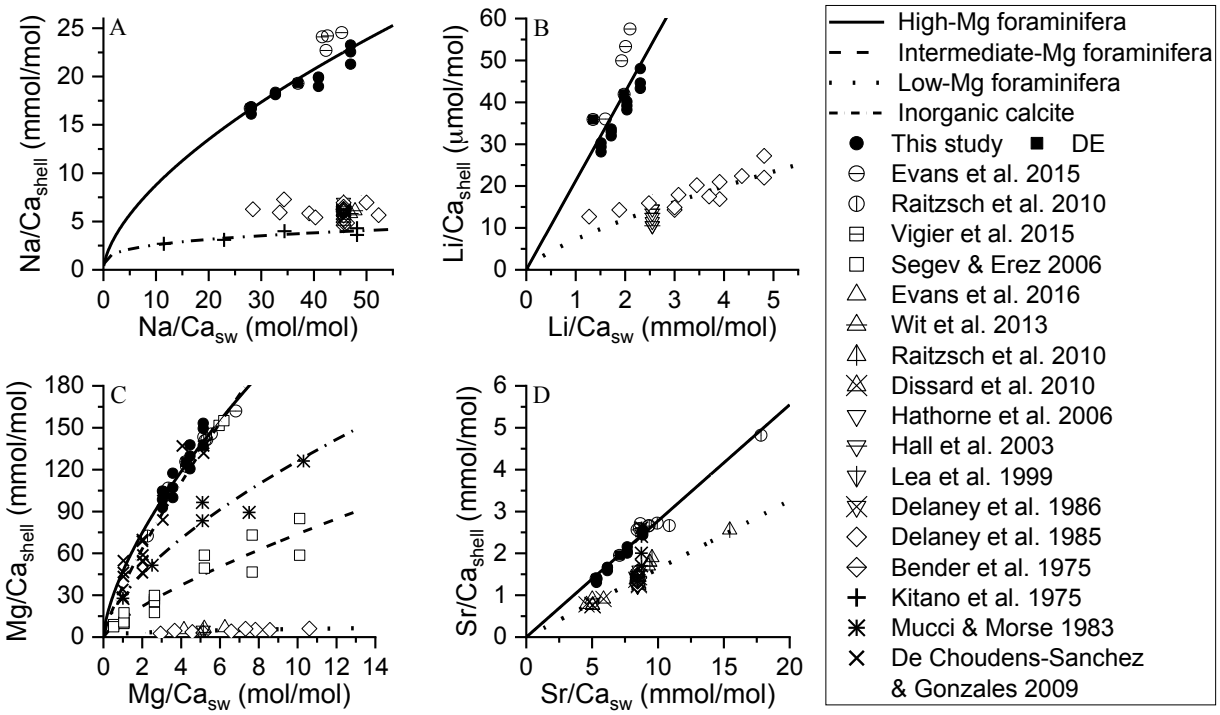

Figure 6: Elements to Ca ratios versus the respective ratio in seawater. Comparison between our data and other foraminifera and inorganic calcite experimental data from the literature (Evans et al. 2015; Raitzsch et al. 2010; Vigier et al. 2015; Segev & Erez 2006; Evans et al. 2016; Evans et al. 2015; Wit et al. 2013; Dissard et al. 2010; Hathrone et al. 2006, Hall et al. 2003, Lea et al. 1999; Delaney & Boyle 1986; Delaney et al. 1985; Bender et al. 1975; Mucci & Morse 1983; Kitano et al. 1975). Power fit equations and their respective R^2 are given below (see figure 7 for the distribution functions).

	High Mg		*Intermediate Mg*		*Low Mg*		*Inorganic calcite*	
El/Ca	Power fit ($\cdot 10^{-3}$)	R^2	Power fit ($\cdot 10^{-3}$)	R^2	Power fit ($\cdot 10^{-3}$)	R^2	Power fit ($\cdot 10^{-3}$)	R^2
Na/Ca	$y=2.10 \cdot x^{0.621}$	0.74			No fit		$y=1.36 \cdot x^{0.280}$	0.76
Li/Ca	$y=21.3 \cdot x$	0.66			$y=0.00726 \cdot x^{0.729}$	0.70		
Mg/Ca	$y=47.2 \cdot x^{0.664}$	0.93	$y=13.1 \cdot x^{0.751}$	0.89	$y=2.51 \cdot x^{0.365}$	0.24	$y=29.3 \cdot x^{0.634}$ $y=36.3 \cdot x^{0.805}$	0.94 0.93*
Sr/Ca	$y=0.278 \cdot x$	0.96			$y=0.163 \cdot x$	0.88	No fit	

* De Choudens-Sanchez & Gonzalez, 2009

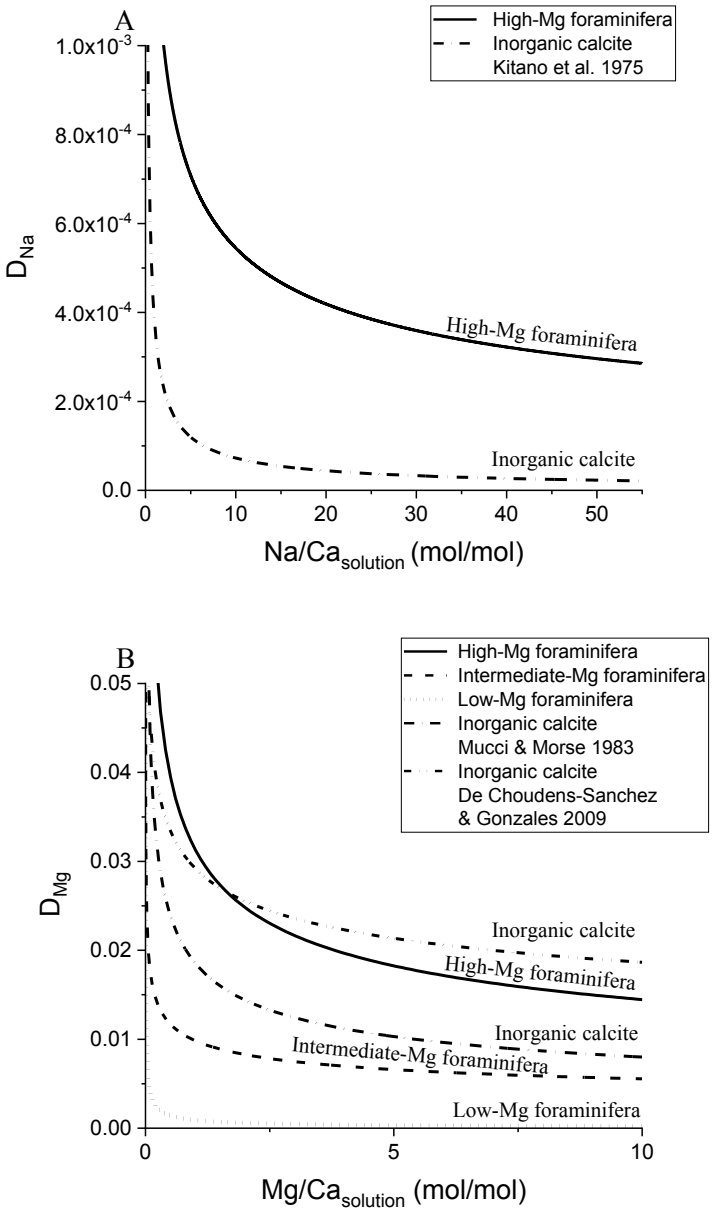

Fig 7: Distribution functions for Na and Mg calculated as the derivative of the power functions in Fig. 6 A and C. The low-Mg data from Raitzsch et al. 2010, Wit et al. 2013, Delaney 1985, Dissard et al. 2010, Lea et al. 1999, Evans et al. 2016, Segev and Erez 2006, Bender et al. 1975.

Study	Derivative of the power fit to the Na/Ca_{shell} vs Na/Ca_{sw}	Derivative of the power fit to the Mg/Ca_{shell} vs Mg/Ca_{sw}
High-Mg foraminifera	$D_{Na}=1.30\cdot10^{-3} \times (Na/Ca_{sw})^{-0.379}$	$D_{Mg}=31.4\cdot10^{-3} \times (Mg/Ca_{sw})^{-0.336}$
Intermediate-Mg foraminifera Segev & Erez 2006		$D_{Mg}=9.84\cdot10^{-3} \times (Mg/Ca_{sw})^{-0.249}$
Low-Mg foraminifera	No fit	$D_{Mg}=0.916\cdot10^{-3} \times (Mg/Ca_{sw})^{-0.635}$
Inorganic calcite-Kitano et al. 1975	$D_{Na}=0.381\cdot10^{-3} \times (Na/Ca_{sw})^{-0.72}$	

Mucci & Morse 1983-Inorganic calcite	$D_{Mg} = 18.6 \cdot 10^{-3} \times (Mg/Ca_{sw})^{-0.366}$
De Choudens-Sanchez & Gonzalez 2009-Inorganic calcite	$D_{Mg} = 29.2 \cdot 10^{-3} \times (Mg/Ca_{sw})^{-0.195}$